JOURNAL OF MATERIALS SCIENCE **37** (2002) 4493–4498

A micro-mechanism based analysis for size-dependent indentation hardness

Y. X. GAO, H. FAN*
Center for Mechanics of Micro-Systems, School of Mechanical and Production Engineering, Nanyang Technological University, Singapore 639798, Singapore
E-mail: mhfan@ntu.edu.sg

A micro-scale analytical model for predicting size-dependent microhardness is presented. The indentation size effect is explained by dissipation energy associated with the contact surfaces. Micro-mechanics mechanism of this energy dissipation is studied via a plastic deformation analysis of micro-scale asperities on the contact surface under indentation. The analysis shows that the microhardness depends not only on the properties of the bulk material under test, but also the properties of the contact surface, such as the plastic behavior of the micro-asperities on contact surfaces. The dependence of microhardness on the roughness parameters of the contact surfaces is also revealed from the analysis.

1. Introduction

It is widely accepted that indentation hardness test is one of the most valuable experimental techniques for measuring mechanical properties of materials. Recently, more attention has been paid to the microhardness indentation tests or nanoindentation techniques [1–3] due to their feasibility to evaluate properties of micro-scale materials/structures used for fabrication of micro-electron-mechanical systems (MEMS) components. Since the properties of the micro-scale materials/structures differ from those in the macro world [4] and MEMS components are too small to be measured by conventional methods, micro/nano indentation tests are probably one of the most feasible techniques to assess mechanical properties of microscopic materials/structures.

Traditionally, the indentation hardness is related to the yield stress of the material under testing. According to the conventional theory of plasticity, the measured hardness value should be a material constant, independent of indenter size or load applied on the indenter as discussed in [5, 6]. On a macroscopic scale, the hardness value is indeed a material constant, which is called true hardness or macrohardness [6, 7]. However, on a microscopic scale, experimental evidence (see, e.g., [1, 2, 8–10]) shows that the measured micro-hardness is no longer a single material constant, but a function of the indenter size, the applied test load, or the depth of the indentation. This is the so-called indentation size effect (ISE). The hardness of thick, high-purity, epitaxially grown silver on sodium chloride was found to be size dependent as the indentation sizes were below $\sim 10\ \mu$m [8]. The Vickers hardness of annealed aluminum varied with applied load in low-load range (between 10 g and 1 kg) [9]. This size-dependent effect of microhardness implies a serious problem for utilization of micro/nano-indentation tests in MEMS characterization, since it is insufficient to quote a single hardness number. Therefore, it is necessary to understand the fundamental physical issues and the parameters involved in micro/nano indentation tests.

The understanding of ISE is still in a stage of development. Explanation of ISE was made by various mechanisms, including the Meyer law [1, 11] and its generalized approaches (see, e.g., [12, 13]) to fit the measured hardness-load or hardness-indentation size data, energy-balance consideration [13, 14], the proportional specimen resistance (PSR) model [1, 7, 12] and so on. Readers are referred to the papers by Li *et al.* [1] and Quinn and Quinn [13] for more models and detailed reviews. Some recent works [6, 8, 15] were especially interested in theoretical prediction and the physical basis of the indentation size effect. Begley and Hutchinnson [6] determined the effect of material length scale on predicted hardness for microindentation tests and explained the ISE by the so-called strain gradient plasticity theory. Nix and Gao [15] studied the ISE in crystalline materials as a law of strain gradient plasticity. In addition, Gerberich *et al.* [16] discussed material property variation with depth, and Bobji and Biswas [17] presented a roughness dependency model for hardness based on single asperity contact. The errors associated with nanoindentation measurement were discussed by Mencik and Swain [18].

In the present paper, the size effect in microhardness tests is argued by dissipation energy associated with the contact surfaces on a microscopic scale. Instead of considering the problem on macro-scale only, we examine

*Author to whom all correspondence should be addressed.

it on both macro and micro scales. Our macro-scale energy analysis shows that total energy consumed during the indentation consists of two parts. The first part is bulk plastic deformation energy, which is associated with the volume pressed by indenter. The second part is the contact dissipation energy, which is directly proportional to the area in contact between the indenter and the material under testing. The ratio of the second part to the first part is negligibly small for a large size indention. The second part only becomes important in micro-indentation tests. On a micro-scale, the mechanism of the contact dissipation energy is studied via a plastic deformation analysis of the asperities. The relationship between the density of contact dissipation energy and the micro-scale roughness parameters of the contact surfaces is established by a statistical analysis for the contact of rough surfaces. As a result, the microhardness and the micro-scale roughness parameters are related in our analysis.

2. Energy balance for indentation

Let us consider a typical static indentation test as shown in Fig. 1, where a rigid indenter with conical shape is firstly pressed into the material under testing by a normal load, and then the normal load is removed. The area of the indentation is measured, and the hardness number is defined by the ratio of the load over the projected area of indentation. With an infinitesimal indentation δx, which is an infinitesimal permanent displacement in the direction of the normal load P, the energies involved in this indentation system changes. Among all the energies, the first term is the work supply to the system by the normal load P, denoted by W; and the second term is the plastic work done in the bulk material, denoted by E_p. On top of these two terms, we introduce a new term E_c that stands for the contact dissipation energy associated with contact surface S_c between the indenter and the material under test, as shown in Fig. 1. Detail derivation of this term is given in the following sections. The last term is sum of all surface energies on the indenter surface and the tested material surface, denoted by Γ. Associated with the indentation δx, the requirement of energy conservation leads to an equation among the changes of these energies, i.e.,

$$\delta W = \delta E_p + \delta E_c + \delta \Gamma \tag{1}$$

It should be emphasized that the elastic deformation energy in the system is released during unloading phase, and therefore no elastic energy change is included in Equation 1.

During the indentation, microscopic asperities on the contact surfaces must deform and change their shapes and distribution under the indentation load, because the force resulted the bulk deformation is transmitted through the microscopic asperities on the contact surfaces. The energy consumed by all the irreversible changes that occur among the microscopic asperities on the two contact surfaces is called the contact surface dissipation energy. Since this contact dissipation energy is only related to the contact surface, but not to the bulk material, it can be expressed as $E_c = A_c e_c$, in which A_c is the area of contact surface S_c, and e_c is called density of dissipation energy per contact area on S_c. On the macro-scale, the density e_c is used as a phenomenological parameter, to be determined by comparing the model predictions with experimental observations. On the micro-scale, it can be directly obtained by micro-scale analysis of the asperity plastic deformation on the contact surface as discussed later. In addition, the interface energy between indenter and material contributes to e_c. The sum of the surface energies on the indenter surface S_i and the tested material surface S_m, shown in Fig. 1, is expressed as $\Gamma = A_i\gamma_i + A_m\gamma_m$ with A_i and A_m as the areas of the surfaces S_i and S_m, and γ_i and γ_m the surface energy densities of the surfaces S_i and S_m. Both γ_i and γ_m are assumed to be material constants in the present analysis.

Let us consider the geometric configuration illustrated in Fig. 1. Associated with the infinitesimal indentation δx, the area changes of the surfaces S_c, S_i and S_m are given by the following equations due to the geometric self-similarity of the indenter,

$$\delta A_c = \frac{2\pi r \delta x}{\sin\theta}, \quad \delta A_i = -\frac{2\pi r \delta x}{\sin\theta}, \quad \delta A_m = -\frac{2\pi r \delta x}{\tan\theta} \tag{2}$$

where r and θ are the radius of the projected area and the angle between material surface and lateral surface of indenter respectively. Meanwhile, the change of plastic work, E_p, done in the bulk test material can be expressed as

$$\delta E_p = \pi r^2 H_0 \delta x \tag{3}$$

based upon the conventional plasticity analysis [5, 10], where H_0 is the macrohardness [6, 7] closely related to the plastic yielding stress of the material. Also, the work supply to the system by the testing load P is

$$\delta W = P\delta x \tag{4}$$

With the help of Equations 2–4, Equation 1 is rewritten as

$$P\delta x = \left(\pi r^2 H_0 \delta x\right) + \left(\frac{2\pi r e_c \delta x}{\sin\theta} - \frac{2\pi r \gamma_i \delta x}{\sin\theta} - \frac{2\pi r \gamma_m \delta x}{\tan\theta}\right) \tag{5}$$

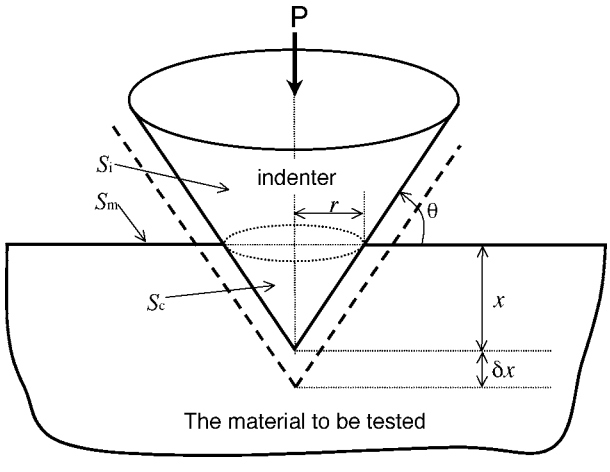

Figure 1 A typical static indentation test.

From Equation 5, it is clear that the work done by the indentation load activates two irreversible mechanisms. The first part is consumed by the plastic deformation in the bulk volume of test material, which is in the order of $O(r^2\delta x)$; and the second part is dissipated by contact surfaces and the changes of surface energy, and in the order of $O(r\delta x)$. An order-of-magnitude analysis of the above two parts shows that the ratio of the second part to the first part is $O(1/r)$. Therefore, the second part can be neglected for a large r. However, in the case of small r, the second part may be of the same order of magnitude with the first part, and cannot be neglected. Therefore, the second part is important in micro-indentation test, and it may be one of the major sources for the indentation size effect.

From Equation 5, it is easy to relate the indentation load and the indentation size, that is

$$P = (\pi H_0)r^2 + \frac{2\pi}{\sin\theta}(e_c - \gamma_i - \gamma_m \cos\theta)r \qquad (6)$$

or

$$P = a_1 r + a_2 r^2 \qquad (7)$$

Constants a_1 and a_2, as the system parameters, depend on the test material properties and the indenter shape, but not on the test load and the indenter size. Quinn and Quinn [13] indicated that a good empirical fit to experimental hardness-load data was obtained by using Equation 7. Hirao and Tomozawa [19] attempted to correlate surface energy to the term $a_1 r$ in Equation 7. Li and coworkers [1, 7, 12] related this term to frictional and elastic contributions in their PSR model. Fracture energy dissipation in ceramic indentation test was also discussed in Quinn and Quinn's work [13]. All above-mentioned mechanisms may make contribution to e_c, the contact surface dissipation energy. But we derived the relation (7) from energy conservation with a concept of density of contact dissipation energy per contact area, not from the fitting of experimental data.

Based on the above analysis, the microhardness or apparent hardness, defined as $H = P/(\pi r^2)$, is given by rewriting Equation 6 as

$$H = H_0 + \frac{2}{\sin\theta}(e_c - \gamma_i - \gamma_m \cos\theta)\frac{1}{r} \qquad (8)$$

It is clear that microhardness H depends on the indentation size r, and increases rapidly when r decreases to zero. Therefore, the second term in Equation 8, contributed by the dissipation energy on contact surfaces, is the reason for the indentation size effect in micro/nano indentation test. Meantime, the fact that $H = H_0$, when $r \to \infty$ implies the measured hardness on macro-scale is indeed a material constant, namely, the macrohardness. Moreover, Equation 8 can be expressed as

$$\frac{H}{H_0} = 1 + \frac{C}{r} \qquad (9)$$

where C, an indentation system constant, does not depend on the indentation size, rather depends on the shape of indenter and more importantly depends on the properties of contact surface between the indenter and test material. It should be pointed out that Equation 9 holds for any self-similar indenter, although it is derived for a conical indenter. From the viewpoint of the phenomenological method, Equation 9 can be used as a prediction for indentation microhardness with a constant C to be determined by experimental data. For example, a set of indentation hardness data of Atkinson [9] on soft metal is predicted by Equation 9 with $C = 4.39\ \mu$m (see Fig. 5). The comparisons show that the prediction is in good agreement with the data. But our effort of modeling does not stop at this point; we look into the micro-scale mechanism for the contact surface dissipation energy e_c. In the following section, we extend the analysis to connect e_c and the micro-scale roughness of contact surfaces.

3. Micro-scale mechanism

At the first glance, an indentation test is pressing an indenter into a flat surface of the material under test. A closer examination of the flat surface, even after the most careful finishing, shows that it is still rough on a relative microscopic scale. Therefore, the contact between the indenter and the testing material is the contact of two rough surfaces on micro-scale, as illustrated in Fig. 2, where a macro-scale contact element and possible interacting asperities within this element on micro-scale are showed schematically.

Although there are many micro-scale mechanisms that can cause dissipation energy at the interacting rough surfaces, we believe that the plastic deformation energy of the micro-asperities on contact surfaces is one of the major parts of the contact dissipation energy. In present study, we only focus on plastic deformation of asperity. Fracture may occur when there are relative motions of interlocking asperities, but the energy dissipation related to fracture is small in comparison with those due to plastic deformation in most cases of indentation test for metals. Elastic deformation energy is also required in indentation test, most of this energy is recoverable and elastic energy losses due to hysteresis are also negligible compared with the energy dissipated by plastic deformation.

Let us recall some of the existing results in contact mechanics of two rough surfaces on the micro scale, which is of fundamental importance to the study of friction, wear and lubrication. Many researchers (see, e.g.,

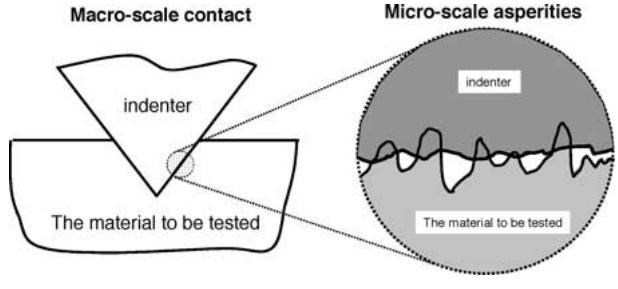

Figure 2 A macro-scale element on contact surface and the possible interacting asperities on the element on micro-scale.

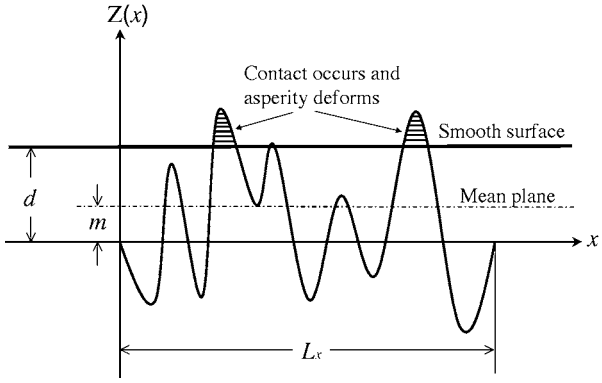

Figure 3 The micro-scale profile of a rough surface.

[20–25]) have studied it. In the present study, we adopt Chang's model [21] directly to carry out the estimation of e_c. Since the contact of two rough surfaces can be modeled as contact between an equivalent rough surface and a flat hard plane [23], we only consider the contact of a single rough surface with an ideal smooth rigid surface. Consider the micro-scale profile of a rough surface as shown in Fig. 3. The surface profile of a representative surface element is expressed as $\{z(x, y); x \in [0, L_x], y \in [0, L_y]\}$, where $z(x, y)$ is the roughness measurement, in which profile heights are measured from a reference plane, the x-axis in Fig. 3; and L_x, L_y are the dimensions of the representative surface element. From the roughness measurement $z(x, y)$ with a given surface element, roughness parameters, such as the mean height, m, and the standard deviation of the rough surface, σ, are defined to characterize the rough surface (see [23]). It is worthwhile to mention that the continuous mechanics concept requires that the area of the surface element is so small on the macro scale that it can be a geometric point on the contact surface considered. Meanwhile, it must be large enough on the micro scale to include so many asperities that the physical properties of this material point can be obtained statistically from the asperities on the surface element. In other words, the roughness parameters, such as m and σ, are independent of the position of the surface element as the dimension of the element is large enough for a homogeneous rough surface.

According to the elastic–plastic model proposed by Chang *et al.* [21], we need the following parameters of the asperities to estimate e_c: (1) the flow pressure of asperity material, p_0, which is a material constant closely related to the macrohardness; (2) the Hertz elastic modulus E, which is related to the Young's modulus E_1 and Poisson's ratio ν_1 of the asperity material as $E = E_1/(1 - \nu_1^2)$; (3) the number density η of asperity; (4) the asperity height distribution function $\phi(z)$; (5) the radius R of asperity summit, which is taken as the statistic average radius of all asperity summits. Another important parameter is the critical interference ω_c, which is expressed as $\omega_c = R(\pi p_0/2E)^2$. As the smooth surface approaches the rough surface, the current separation between the smooth surface and the reference plane is denoted by d. For any given d, all asperities whose heights are originally greater than d must be in contact with the smooth surface, as shown in Fig. 3. The real contact area for unit nominal surface area is given by the Chang's model [21] as

$$A_r(d) = A_e(d) + A_p(d) \tag{10}$$

with

$$A_e(d) = \eta\pi R \int_d^{d+\omega_c} (z-d)\phi(z)\,dz \tag{11}$$

$$A_p(d) = \eta\pi R \int_{d+\omega_c}^{\infty} [2(z-d) - \omega_c]\phi(z)\,dz \tag{12}$$

The total load for the unit nominal surface area is given by

$$P(d) = \frac{4}{3}\eta\pi E R^{1/2} \int_d^{d+\omega_c} (z-d)^{3/2}\phi(z)\,dz + p_0 A_p(d) \tag{13}$$

Assume the volume conservation of the micro-asperities during deformation process, the total plastic work is contributed by the plastic deformation of asperities when the smooth surface approaches from $d = \infty$ to $d = m$. Actually, the volume of the asperities above the mean plane is equal to that below the mean plane, and the rough surface becomes smooth when the smooth surface approaches to the mean plane, namely when $d = m$. Based on this assumption, with the help of Equations 12 and 13, the dissipation energy per unit nominal contact surface due to the plastic deformation of asperities on micro-scale is given as,

$$e_c = \eta\pi R p_0 \int_m^{\infty} \int_{d+\omega_c}^{\infty} [2(z-d) - \omega_c]\phi(z)\,dz\,dd \tag{14}$$

Generally, it is difficult to give an analytical expression of asperity height distribution function $\phi(z)$ in Equation 14 for a real rough surface. In order to demonstrate our model, hereby we consider an exponential distribution,

$$\phi(z) = \frac{1}{\sigma}\exp\left(-\frac{z-m}{\sigma}\right) \tag{15}$$

It is a good approximate for many practical rough surfaces, including the Gaussian distribution surfaces [24]. In this case, combination of Equations 14 and 15 gives

$$e_c = \eta\pi R p_0 \sigma(2\sigma + \omega_c)\exp\left(-\frac{\omega_c}{\sigma}\right) \tag{16}$$

From Equation 14 and its special case (16), the density of contact dissipation energy due to plastic deformation of micro-asperities on the rough surfaces depends both on the material properties $\{p_0, E\}$ of the micro-asperities and the roughness parameters $\{\sigma, \eta, m, R\}$ of the rough surfaces. For a given surface, since all these parameters can be measured, the density of contact surface dissipation energy, e_c, is therefore determined. It can be seen that rougher and softer surfaces have higher densities of contact surface dissipation energy.

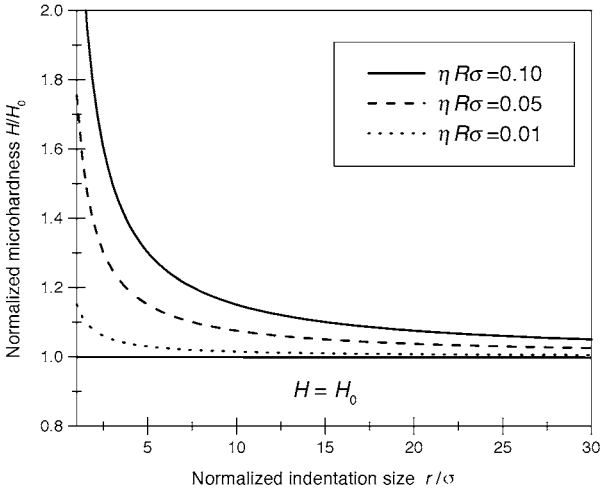

Figure 4 The influence of roughness parameters on microhardness.

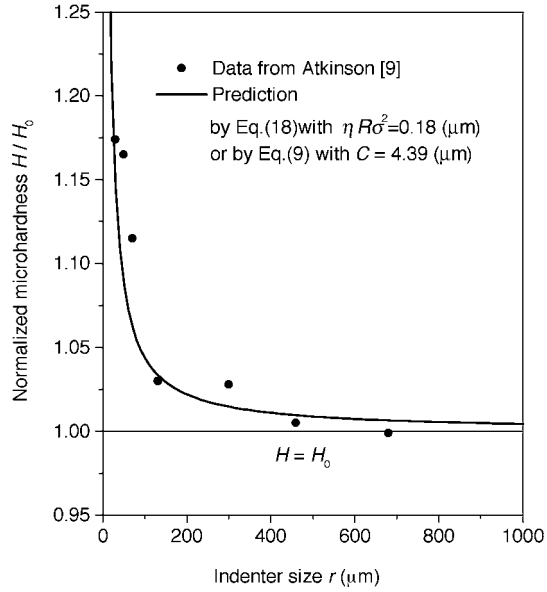

Figure 5 The dependence of microhardness on the indentation size.

Moreover, a combination of Equations 8 and 16 gives

$$H = H_0 + \frac{2}{\sin\theta}[\eta\pi Rp_0\sigma(2\sigma + \omega_c)\exp(-\omega_c/\sigma) - \gamma_i - \gamma_m\cos\theta]\frac{1}{r} \quad (17)$$

Clearly, from Equation 17, the microhardness depends both on the micro-scale surface roughness parameters and the properties of micro-asperity.

For soft metals, such as aluminum and mild steel, the critical flow pressure of asperity material p_0 can approximately be related to macrohardness H_0 as $p_0 = 0.6H_0$ (see, [21]), and the elastic deformation is too small to be taken into account, namely $\omega_c = 0$. The influence by surface tensions γ_i and γ_m is also negligible [19].

Therefore, Equation 17 can be simplified as

$$\frac{H}{H_0} = 1 + \frac{2.4\pi}{\sin\theta}(\eta R\sigma)\frac{1}{r/\sigma} \quad (18)$$

It is clear that the microhardness depends on the surface roughness parameter group ($\eta R\sigma$). Fig. 4 shows how this grouped parameter affects the relationship between normalized microhardness and normalized indenter size by the standard deviation σ of the contact surface. In Fig. 4, a value of $\theta = 18^\circ$ is selected, which corresponds to a Vickers indenter (see [6]). It also can be seen from Fig. 4 that rougher surfaces have stronger size dependence in indentation test.

A set of microhardness test data for aluminum specimen from Atkinson [9] is shown in Fig. 5, where the microhardness is plotted against the indentation size. The prediction given by Equation 18 is also illustrated by solid line in Fig. 5, in which the value of angle θ is taken to be 18 degrees according to a Vickers indenter (see [6, 9, 26]). From Fig. 5, it is clear that the prediction with the roughness parameters taken as $\eta R\sigma^2 = 0.18$ μm is in good agreement with the experimental data from Atkinson [9]. Unfortunately, there is no surface roughness data cited in Atkinson's experiment. However, they indicated in their papers [9, 26] that the microhardness data were measured on an annealed aluminum surface polished to metallographic standard. Greenwood and Williamson [20] gave a set of physically reasonable roughness data for nominally flat surfaces, in which $\eta = 300/\text{mm}^2$, and $R\sigma = 10^{-4}$ mm^2. They also indicated that for polished flat surfaces the value of R is in the range of 10–100 μm. Based on these data, the value of $\eta R\sigma^2$ for polished surfaces should be in the range between 0.03 μm and 0.3 μm. Nuri and Halling [25] measured these roughness parameters of mild steel surfaces that were ground and lapped, where σ is in the range of 0.131–4.978 μm, R of 18.364–5.842 μm, and η from 0.033/μm^2 to 0.009/μm^2. According to their measurement, the value of $\eta R\sigma^2$ is in the range of 0.010–1.303 μm. On the basis of the above-mentioned surface roughness data, we can conclude that the value, $\eta R\sigma^2 = 0.18$, used in our prediction is in a practically reasonable range for polished surfaces.

4. Summary

This paper presents a new micro-mechanics model for predicting the size-dependent microhardness, and suggests that the indentation size effect may be caused by the contact dissipation energy associated with the contact surface. An explicit form of contact dissipation energy is derived by considering plastic deformation of the micro-scale asperities on the contact surfaces.

The indentation microhardness is dependent on both plastic work of the bulk material under test and the contact dissipation energy associated with the contact area. For large size indentation, the contact dissipation energy is very small in comparison with the bulk plastic work, thus can be ignored. As the result, the measured macrohardness is a material constant that depends only on the bulk property of the test material. For micro/nano indentation, the contact dissipation energy may be of the same order of magnitude with bulk plastic work, and therefore cannot be neglected. The microhardness is seen as a function of the indentation size.

It is noticed that all the micro-hardness experimental data were obtained without quote of surface roughness information. Therefore, it is necessary that further micro-indentation tests with real material constants and controlled surface roughness parameters are needed to qualify the present model quantitatively.

References

1. H. LI and R. C. BRADT, *J. Mater. Sci.* **28** (1993) 917.
2. M. ATKINSON, *ibid.* **30** (1995) 1728.
3. M. GOKEN and M. KEMPF, *Acta Mater.* **47**(3) (1999) 1043.
4. E. MAZZA and J. DUAL, *J. Mech. Phys. Solids* **47**(8) (1999) 1795.
5. D. TABOR, in "Microindentation Techniques in Materials Science and Engineering," edited by P. J. Blau and B. R. Lawn, ASTM STP889 (American Society for Testing and Materials, Philadelphia, PA, 1986), p. 129.
6. M. R. BEGLEY and J. W. HUTCHINSON, *J. Mech. Phys. Solids* **46** (1998) 2049.
7. A. IOST and R. BIGOT, *J. Mater. Sci.* **31** (1996) 3573.
8. Q. MA and D. R. CLARKE, *J. Mater. Res.* **10**(4) (1995) 853.
9. M. ATKINSON, *ibid.* **10**(11) (1995) 2908.
10. N. P. SUH, in " Tribophysics" (Prentice-Hall, Englewood Cliffs, 1986) p. 39.
11. G. N. BABINI, A. BESSOSI and C. GALASSI, *J. Mater. Sci.* **22** (1987) 1687.
12. H. LI, A. GHOSH, Y. H. HAN and R. C. BRADT, *J. Mater. Res.* **8**(5) (1993) 1028.
13. J. B. QUINN and G. D. QUINN, *J. Mater. Sci.* **32** (1997) 4331.
14. J. GONG, J. WU and Z. GUAN, *Mater. Lett.* **38** (1999) 197.
15. W. D. NIX and H. GAO, *J. Mech. Phys. Solids* **46** (1998) 411.
16. W. W. GERBERICH, S. K. VENKATARAMANAN, H. HUANG, S. E. HARREY and D. L. KOHLSTEDT, *Acta Metall. Mater.* **43** (1995) 1569.
17. M. S. BOBJI and S. K. BISWAS, *J. Mater. Res.* **13** (1998) 3227.
18. J. MENCIK and M. V. SWAIN, *ibid.* **10** (1995) 1491.
19. K. HIRAO and M. TOMOZAWA, *J. Amer. Ceram. Soc.* **70** (1987) 497.
20. J. A. GREENWOOD and J. B. P. WILLIAMSON, *Proc. R. Soc. London, Ser. A* **295** (1966) 300.
21. W. R. CHANG, I. ETSION and D. B. BOGY, *ASME Journal of Tribology* **109** (1987) 257.
22. T. L. WARREN, A. MAJUMDAR and D. KRAJCINOVIC, *J. Appl. Mech.* **63** (1996) 47.
23. A. MAJUMDER and B. BHUSHAN, in "Handbook of Micro/ Nano Tribology," edited by B. Bhushan, 2nd ed. (CRC Press, Boca Raton, 1999) p.187.
24. J. HALLING, in "Principles of Tribology" (Macmillan Press, London, 1978).
25. K. A. NURI and J. HALLING, *Wear* **32** (1975) 81.
26. H. SHI and M. ATKINSON, *J. Mater. Sci.* **25** (1990) 2111.

Received 28 February 2001
and accepted 8 July 2002